



Exergy-Economic analysis of combined cooling, heat and power system utilizing solar energy and biomass

Seyyed Amirreza Abdollahi*  | Seyyed Faramarz Ranjbar
Mir Biuok Ehghaghi | Moharram Jafari

Faculty of Mechanical Engineering, University of Tabriz, Tabriz, Iran

* Corresponding author, Email: s.a.abdollahi@yahoo.com

Article Information

Article Type

RESEARCH ARTICLE

Article History

RECEIVED: 19 Sep 2024

REVISED: 28 Oct 2024

ACCEPTED: 31 Oct 2024

PUBLISHED ONLINE: 17 Nov 2024

Keywords

Solar energy

Biomass

Photovoltaic panel

Multi-objective optimization

Abstract

Industrial advancements in recent years have led to a significant increase in global energy consumption. Consequently, the pollution resulting from the use of fossil fuels to meet this energy demand has become a pressing issue. The utilization of biomass as a renewable energy source presents a viable solution to mitigate this problem. In addition to biomass, solar energy has also emerged as a dependable energy source that has been extensively researched in recent times. This study proposes a combined cooling, heat and power (CCHP) system that integrates four different systems - biomass, milk powder processing, refrigeration, and photovoltaic panels to generate electricity, milk powder, and cooling capacity. The proposed system underwent optimization through multi-objective approach to enhance its overall performance and payback period time. The findings indicate that the payback period for the investment can be reduced to 3.82 years, with a maximum cycle efficiency of 33 percent. These values can be adjusted based on the relative importance of each factor. For instance, if the payback period is extended to 4.8 years, the cycle efficiency would decrease to 27 percent.

Cite this article: Abdollahi, S. A., Ranjbar, S. F., Ehghaghi, M. B., Jafari, M., (2024). Exergy-Economic analysis of combined cooling, heat and power system utilizing solar energy and biomass. DOI: [10.22104/hfe.2024.7058.1311](https://doi.org/10.22104/hfe.2024.7058.1311)



© The Author(s).

Publisher: Iranian Research Organization for Science and Technology (IROST)

DOI: [10.22104/hfe.2024.7058.1311](https://doi.org/10.22104/hfe.2024.7058.1311)

1 Introduction

The rapid industrial, economic, and societal advancements, coupled with the increasing global population, have led to a surge in energy demand. To address this ever-growing need for energy, there is a reliance on the utilization of more and more fossil fuels. However, as fossil fuel reservoirs are finite and expected to deplete in the near future, there is an urgent need to explore and develop new energy sources and systems. Furthermore, the environmental impacts resulting from the use of fossil fuels, such as irreversible pollution, necessitate a shift towards reducing emissions of pollutants like carbon dioxide, nitrogen oxides, sulfur dioxide, and particles by minimizing the dependency on fossil fuels [1, 2]. The majority of renewable energy sources stem from solar energy, with the exceptions be-

ing geothermal, nuclear, and tidal. In recent years, renewable energy sources have emerged as viable alternatives to fossil fuels. Unlike fossil fuels, these energy sources do not have the same environmental impacts, making them a compelling choice for energy production. Biomass, for example, is a type of fuel that is generated through the anaerobic digestion of agricultural, food, forestry, wastewater, and animal waste [3]. The primary objective of advancing novel techniques in energy systems is to enhance the efficiency of the system, boost production, and minimize the release of harmful pollutants. One promising approach to accomplish this objective is through the implementation of a combined cycle of cooling, heat and power (CCHP). These CCHP cycles are highly adaptable and can be employed in various applications with different power ratings. Notably, in recent times, CCHP cycles have found significant utilization in domestic settings. Figure 1 illustrates a CCHP system.

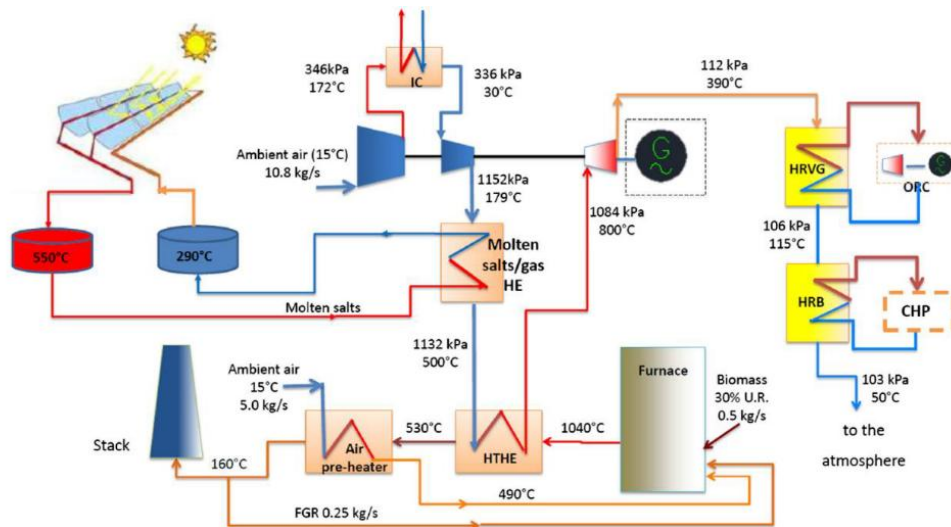


Fig. 1. Biomass-Solar system for combined cycle power plant [4].

Solar power capabilities are clearly visible, but the periodic nature and uncertainty of solar energy will impose limitations on this energy source. Consequently, solar energy must be integrated with other energy sources to guarantee a consistent and dependable energy supply. CCHP Systems can play a crucial role in mitigating the challenges faced by solar energy systems. By utilizing multiple energy sources in conjunction with solar energy, CCHP systems can serve as supplementary sources and contribute to an optimal design for the desired service. Dairy farms, as centers capable of producing power and heat while adding value by converting raw milk into products like powdered milk, represent a new topic that has not previously

been addressed as an integrated system. This study will explore a hybrid system composed of biomass and photovoltaic energy from the perspectives of energy, exergy, economics, and environmental. In other words, the novelty of the present work is that in this research a new cycle is proposed that can utilize the renewable energies like solar and biomass which is produced in the dairy farm to cogenerate heat, power and milk powder which is a high value product.

CCHP systems with different renewable energy sources can lead to large-scale industrial plants or small-scale domestic system. This versatility is a major advantage of such said systems over conventional systems.

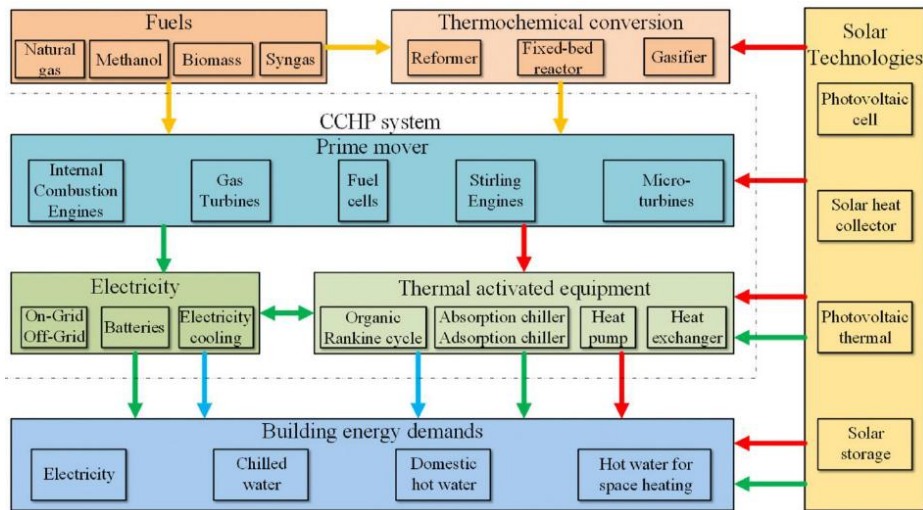


Fig. 2. Energy stream for different CCHP systems of energy.

In a study by Nazari [5] et al. a multi objective optimization of a solar/biomass trigeneration system utilizing a gas turbine, ORC and absorption refrigeration cycle has been studied. They adopted the method of multi-verse optimization for their optimization study. The results of exergo-economic analysis indicated that in design condition the energy and exergy efficiencies

are 55.56% and 20.38% respectively. Also, the cost rate of the cycle product is estimated to be 26.4 \$/h. in the results of multi-objective optimization revealed that the optimized cycle can have 9% higher second law efficiency with 6% lower product cost. The schematic of the cycle proposed in their research is shown in Figure 3.

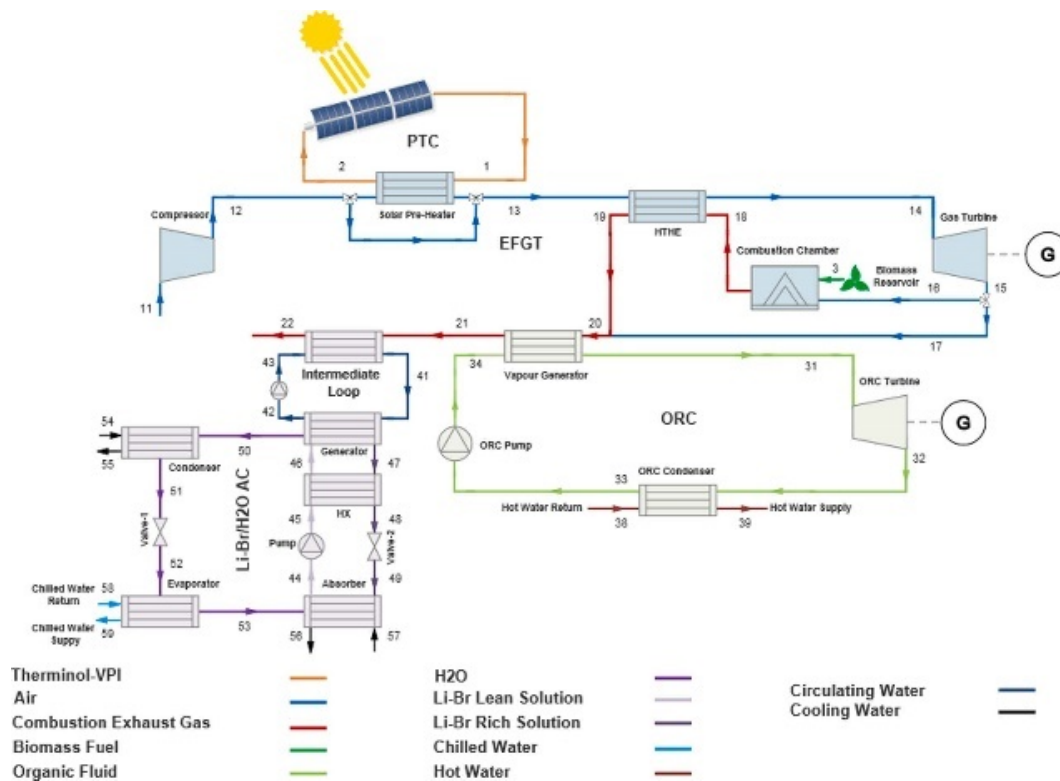


Fig. 3. Schematic configuration of the proposed CCHP plant in Nazari's Work [5].

Based on their Work it can be said that the advantages of integrating solar energy into the proposed trigeneration system are emphasized through a comparison of key performance parameters with existing literature. The results indicate that the proposed system can achieve approximately 17% greater power output, 23% increased cooling load, and nearly double the heating load, with a first law efficiency of 54.25%. Exergy analysis reveals that the solar module and biomass combustor have the highest exergy losses. Additionally, an examination of the exergo-economic factors across different components highlights that the compressor, gas turbine, and heating unit are the least efficient in terms of exergo-economic performance. The parametric study further suggests that the pressure ratio and Gas turbine inlet temperature have a more significant impact on system outputs compared to other decisive variables. Finally, a novel optimization algorithm, called MOMVO, is employed to determine the Pareto frontier of the exergo-economic problem. The optimal solution identified by MOMVO shows that the studied trigeneration system can achieve an exergy efficiency of 22.20%, with a product cost rate of 24.86 \$/h. A comparison of the results obtained from MOMVO with those from MOPSO and NSGA-II demonstrates MOMVO's superior performance in addressing the multi-objective optimization challenges of this study.

In another research conducted by Saini et al [6], Thermodynamic, economic and environmental analysis of a novel solar energy driven small-scale for combined cooling, heating and power system has been conducted.

As the theoretical assessment of the exergy, economic, and environmental performance of the novel Combined Cooling, Heating, and Power (CCHP) system has been conducted, this proposed system consists of four primary cycles: ETC (stationary collector) cycle, TES (for solar intermittence), ORC (low-temperature power cycle), ERC (heat-driven cooling cycle), and a water heater (plate heat exchanger) cycle, enabling the simultaneous generation of cooling, power, and heating outputs.

- The overall exergy efficiency, total cost rate, and equivalent carbon dioxide emission reduction are calculated to be 3.159%, \$2023 per year, and 13.10 tons, respectively.
- The highest percentage of irreversibility is found in the collector at 89.82%, followed by the water heater, ejector, and vapor generator at 2.327%, 1.688%, and 1.33%, respectively.
- Increasing the generator temperature enhances exergy efficiency, CO₂ emissions, and heating costs, while reducing cooling and power costs.
- Raising the condenser temperature leads to a

decrease in exergy efficiency, cooling and power costs, but an increase in heating costs and CO₂ emissions.

- An increase in turbine mass fraction boosts exergy efficiency, power costs, and equivalent carbon dioxide emissions, while reducing cooling costs and the cooling-power cost ratio. The PPTD in the generator is more critical for system cost considerations compared to other heat exchangers.
- Higher exergy efficiency in this CCHP system can be achieved by increasing generator and condenser temperatures and lowering evaporator temperatures. Conversely, a lower system cost per unit of overall output can be attained by increasing the temperatures of the generator, condenser, and evaporator.

Overall, the proposed CCHP system presents a viable alternative for fulfilling energy demands in cooling, heating, and power production.

2 Materials and methods

The flexibility of CCHP systems utilizing various renewable energy sources allows for their application in both large-scale industrial facilities and small-scale residential setups. This adaptability stands as a significant benefit of these systems compared to others. Biomass is composed of various gaseous compounds, predominantly Methane and carbon dioxide [7]. Methane is the primary constituent of biomass. Extensive research has been conducted on biomass in recent years. As indicated by Abdeshahian [8] et al, the electricity generated in Malaysia through Anaerobic digestion of biomass is approximately 8.27 trillion watt hours. Various techniques such as pyrolysis, gasification, and Anaerobic digestion can be utilized for the industrial production of biomass. Anaerobic digestion stands out as a sustainable approach that results in biomass production without generating any byproducts. Additionally, this method requires significantly less space in comparison to alternative methods. Solar heat collectors (SHC) and photovoltaic panels (PVT) have been used in both industrial and domestic applications. Considering the recent developments, solar systems can play a vital role in CCHP systems. Solar systems can be coupled with other systems like wind and other combined energy systems. Combining of such systems can lead to more efficient systems and can be used for many applications such as power, heating and cooling. Solar energy can be stored with energy storage systems and be used for in other energy systems. For example, and biomass-solar along with Brayton cycle has been proposed by Pantaleo et al. [4].

The equations below represent the conservation of energy and exergy destruction rate for every component within the system.

$$\dot{Q}_{CV} - \dot{W}_{CV} = \sum \dot{m}_{out} h_{out} - \sum \dot{m}_{in} h_{in}, \quad (1)$$

$$\dot{E}_D = \sum \dot{E}_{in} - \sum \dot{E}_{out}. \quad (2)$$

In Equation (2), the rate of exergy transfer (\dot{E}) is equivalent to the mass flow rate of exergy ($\dot{m}e$) and is the combination of physical and chemical exergy, where (e) represents the total specific exergy.

$$\bar{e} = \bar{e}^{ph} + \bar{e}^{ch}. \quad (3)$$

Equation (4) enables the computation of the precise exergy of the fluid flow in terms of its physical characteristics.

$$\bar{e}^{ph} = \bar{h} - \bar{h}_0 - T_0(\bar{s} - \bar{s}_0). \quad (4)$$

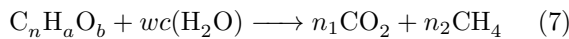
Equation (5) enables the computation of the specific exergy of a chemical substance.

$$\bar{e}^{ch} = \sum_{i=1}^j y_i \bar{e}_i^{ch} + \bar{R}T_0 \sum_{i=1}^n y_i \ln y_i. \quad (5)$$

Equation (5) demonstrates that the rate of exergy destruction is equivalent to the total exergy of the inlet and outlet streams. Exergy efficiency can be determined by utilizing Equation (6).

$$\varepsilon_i = \frac{\dot{E}_{P,i}}{\dot{E}_{F,i}}. \quad (6)$$

During the Anaerobic digestion process, the initial substance undergoes heating to a temperature of 55 °C without the presence of oxygen. By applying the technique established by Buswell and Hatfield [11], one can forecast the composition of the resultant biomass gas. In a broad sense, the chemical reaction involved in the generation of biomass through Anaerobic digestion can be described as follows.



In Equation (7), the subscripts will vary depending on the primary material utilized in the production of biomass.

Table 1. The Component of biomass based on primary material compound [12].

Type of waste	C	H	O	N
Cow waste	38.06	5.18	28.15	1.85
Sheep waste	37.64	5.06	28.64	1.87
Chicken waste	26.77	3.33	30.52	2.25

The Higher heating values for the different types of waste are 16.56, 16.09, and 11.92 MJ/kg, respectively. To determine the chemical exergy of biomass, the empirical relation provided in Equation (8) can be employed, considering the non-homogeneous texture of the biomass [12]

$$e_{manu,daf}^{ch} = LHV_{manu,daf} \times \frac{1.044 + 0.016 \frac{z_H}{z_C} + 0.3493 \frac{z_O}{z_C} (1 + 0.0531 \frac{z_H}{z_C})}{1 - 0.4124 \frac{z_O}{z_C}} \quad (8)$$

In Equation (8), z_H , z_C , z_O are the hydrogen, carbon and oxygen mass fraction in biomass respectively [12].

Joshi et al [10] presented the mathematical equations necessary for the modeling of the solar panel. There are several approaches available for exergy-Economic Optimization, including Exergy cost theory, Average cost approach, and Specific exergy costing. In this particular investigation, the focus is on Exergy cost. This method involves formulating Equation (9) for every component within the system [13–16].

$$\sum \dot{C}_{out,k} + \dot{C}_{W,k} = \sum \dot{C}_{in,k} + \dot{C}_{Q,k} + \dot{Z}_k \quad (9)$$

Equation (9) represents the relationship between the initial capital cost (C) and the cost of using and maintaining (Z) a particular system. Additionally, $\dot{C}_{w,k}$ and $\dot{C}_{Q,k}$ denotes the cost rate of work and heat, respectively. It is possible to calculate all these parameters by utilizing the equations provided below.

$$\dot{Z}_k = \dot{Z}_k^{CI} + \dot{Z}_k^{OM} \quad (10)$$

$$\dot{C}_{in} = c_{in} \dot{E}_{in} \quad (11)$$

$$\dot{C}_{out} = c_{out} \dot{E}_{out} \quad (12)$$

$$\dot{C}_Q = c_Q \dot{E}_Q \quad (13)$$

$$\dot{C}_W = c_W \dot{E}_W \quad (14)$$

Equation (15) can be employed to compute \dot{Z}_k based on the procurement cost of the equipment.

$$\dot{Z}_k = CRF \frac{\phi_r}{N} PEC_k \quad (15)$$

In Equation (15), CRF, N , and ϕ_r denote the cost return factor, annual working hours (assumed as 7880 hours in this study), and maintenance factor (assumed as 1.06 in this study). The exergy-economic equation for each component of the cycle is provided in Table 4. The initial capital costs for each component are listed in Table 5 [13–16].

3 Results and discussion

Firstly, this section will delve into the topic of validation, followed by an examination of the outcomes derived from the modeling and optimization of the cycle. Wellinger’s work [12] is being compared with the current study to validate the findings on biomass production.

Table 2. Validation for biomass production cycle [12].

Chemical Component	Current work	Reference work [12]
CH ₄ (%)	58.4	58
CO ₂ (%)	41.6	42

Behzadi et al [15] study was consulted for validating the outcomes of the biomass and Rankine subsystem. A visual representation of the comparison of the results can be observed in Figure 6.

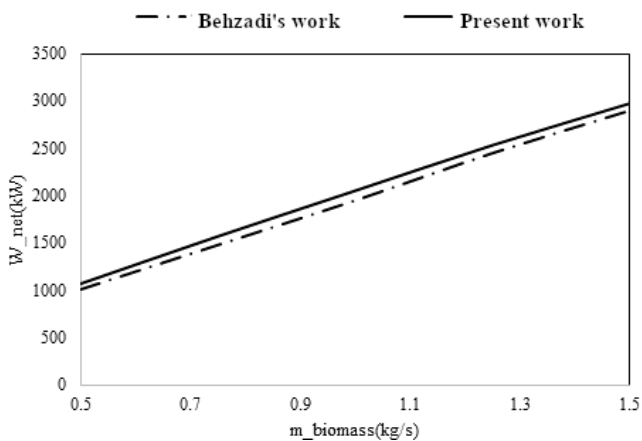


Fig. 6. Validation of biomass and Rankine cycle [15].

Aman’s work [17] will be cited in Figure 7 to confirm the findings of the absorption refrigeration cycle.

The rate of exergy destruction for each component which are calculated in the present work and comparison with reference work of are provided in Table 3.

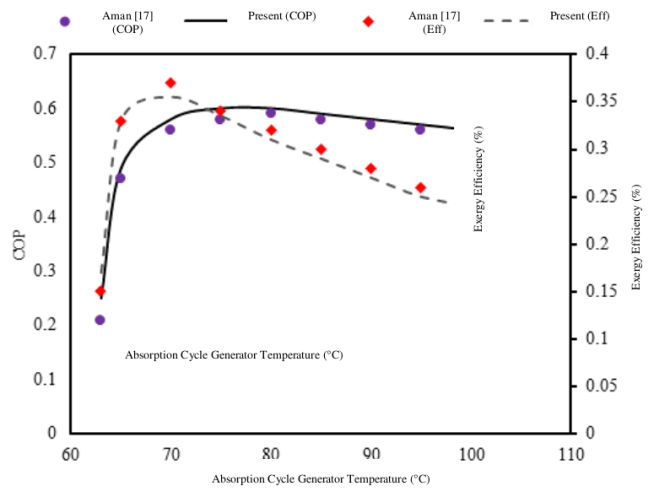


Fig. 7. Validation of absorption refrigeration cycle [17].

In this section since multi-objective optimization will be conducted both parameters of payback period and exergy efficiency will be optimized simultaneously.

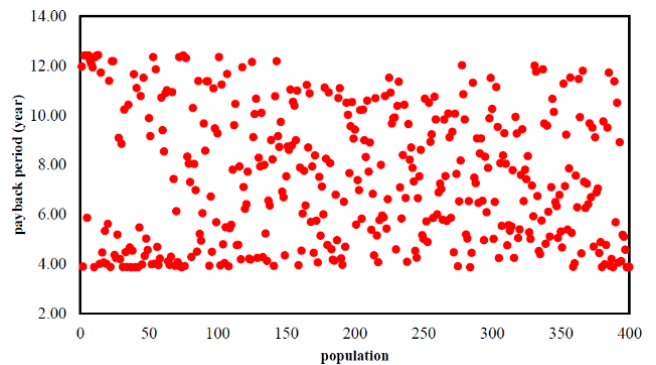


Fig. 8. Results of multi-objective optimization of payback period.

Table 3. Exergy destruction rate for main component of the cycle.

Aim	Payback period	Exergy efficiency (%)	Biomass mass flow rate (kg/s)	Milk powder mas flow rate (kg/s)	Solar panel surface area (m ²)	Cooling capacity (kW)	Combustion chamber inlet temperature (°C)	Turbine inlet pressure
Payback period	3.82	24.7	1.61	2.94	570	20	1185	2200
Optimum exergy efficiency (%)	12.5	33	0.7	2.7	440	180	1400	2500

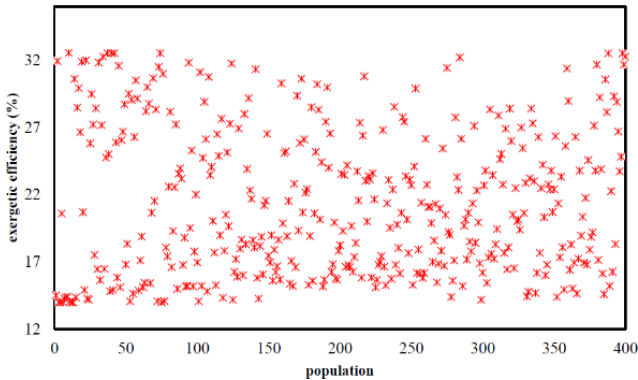


Fig. 9. Results of multi-objective optimization of exergetic efficiency.

Based on the data presented in Figures 10 and 11, it can be observed that the findings suggest an optimized target for the payback period lies within the range of 4 to 9 years. Additionally, the exergy range is projected to be between 18 to 34 percent, respectively.

To simplify the outcomes of multi-objective optimization, one can refer to Figure 10 for a visual representation. By examining Figure 10, it becomes possible

to easily calculate the exergy efficiency and payback period in relation to each other.

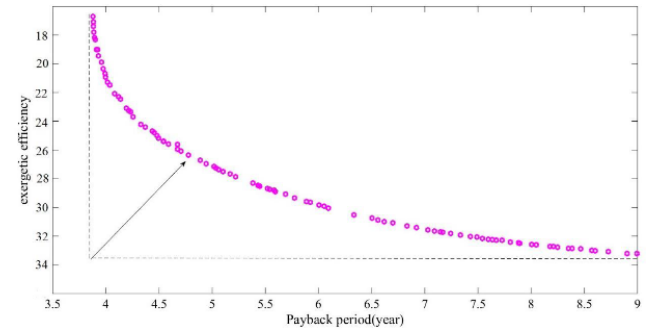


Fig. 10. Results of optimization for exergy efficiency vs. Payback period.

An analysis was conducted on the impact of various parameters, including the rate of biomass consumption, crude milk consumption rate, PVT surface area, temperature of the combustion chamber, cooling capacity of the absorption cycle, and turbine inlet pressure, on both the payback period and exergy efficiency.

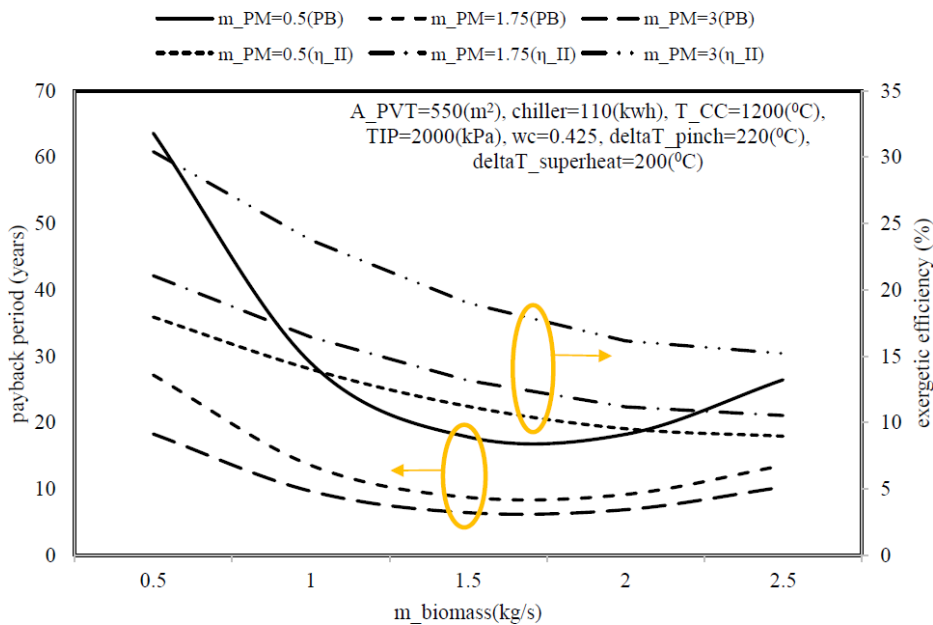


Fig. 11. Impact of biomass consumption and crude milk consumption rate on payback period and exergy efficiency.

Figure 11 illustrates that as the consumption rate of biomass rises, the exergy efficiency will decline. Conversely, reducing the consumption rate of crude milk will also lead to a decrease in efficiency, owing to a lower production rate within the cycle.

As indicated in Figure 12, the surface area of PVT

panels has a negligible effect on the efficiency and payback period of the cycle. This is primarily because the overall efficiency of PVT panels surpasses that of biomass systems, thereby making any changes in the biomass system more apparent.

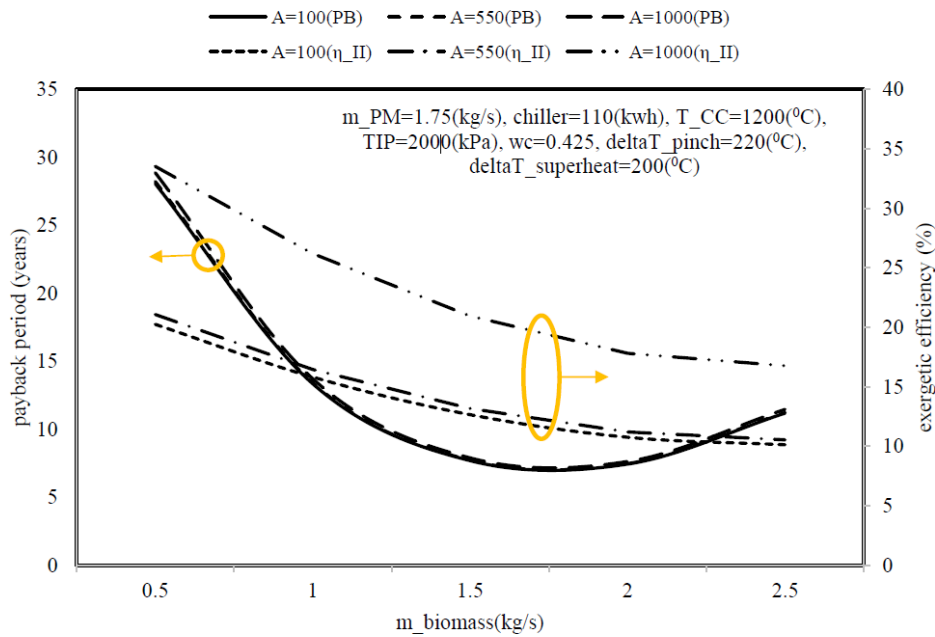


Fig. 12. Impact of biomass consumption and PVT surface area rate on payback period and exergy efficiency.

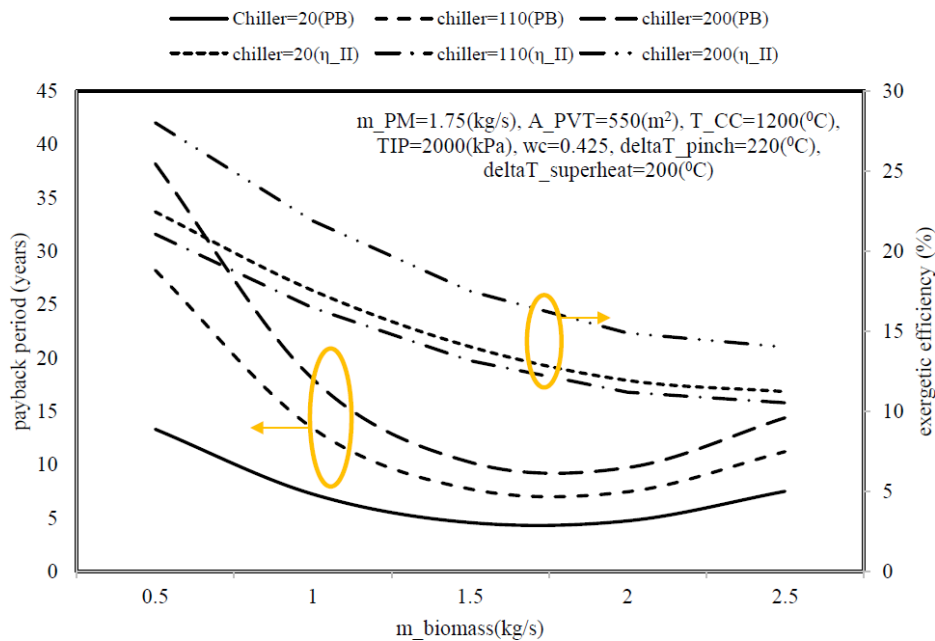


Fig. 13. Impact of biomass consumption and absorptio cycle cooling capacity on payback period and exergy efficiency.

Increasing the cooling capacity of the absorption cycle, as depicted in Figure 13, clearly results in a longer payback period. This highlights the significant expenses associated with producing cooling capacity in the absorption cycle.

Figure 14 illustrates that elevating the temperature within the combustion chamber leads to a slight reduction in the payback period. Moreover, augmenting the temperature enhances the exergy efficiency; however, it

concurrently results in increased costs for the combustion chamber due to the utilization of more advanced technological construction techniques.

By contrasting Figures 14 and 15, it becomes apparent that the impact of combustion chamber temperature surpasses that of turbine inlet pressure when considering exergy efficiency. Conversely, the turbine inlet pressure exhibits a greater influence on the payback period.

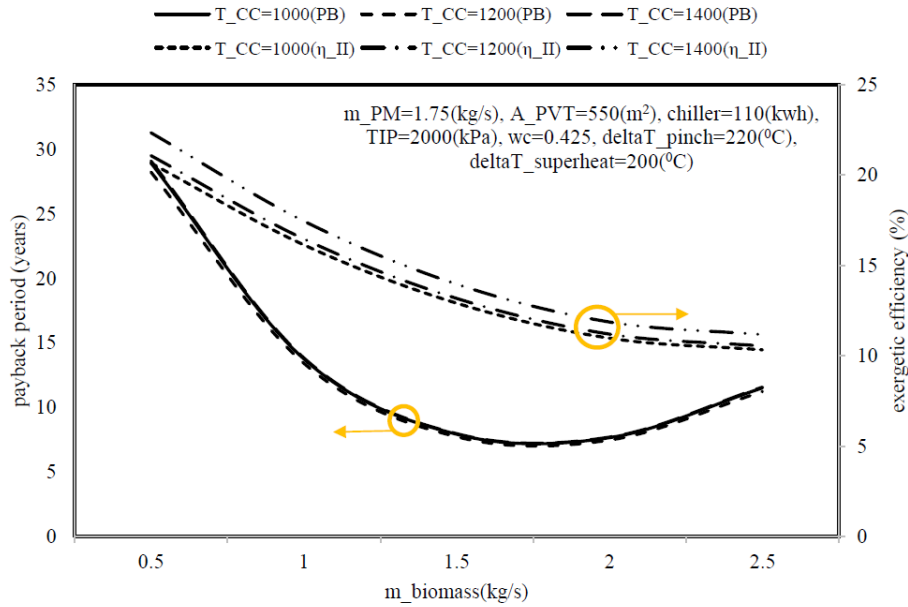


Fig. 14. Impact of biomass consumption and combustion chamber temperature on payback period and exergy efficiency.

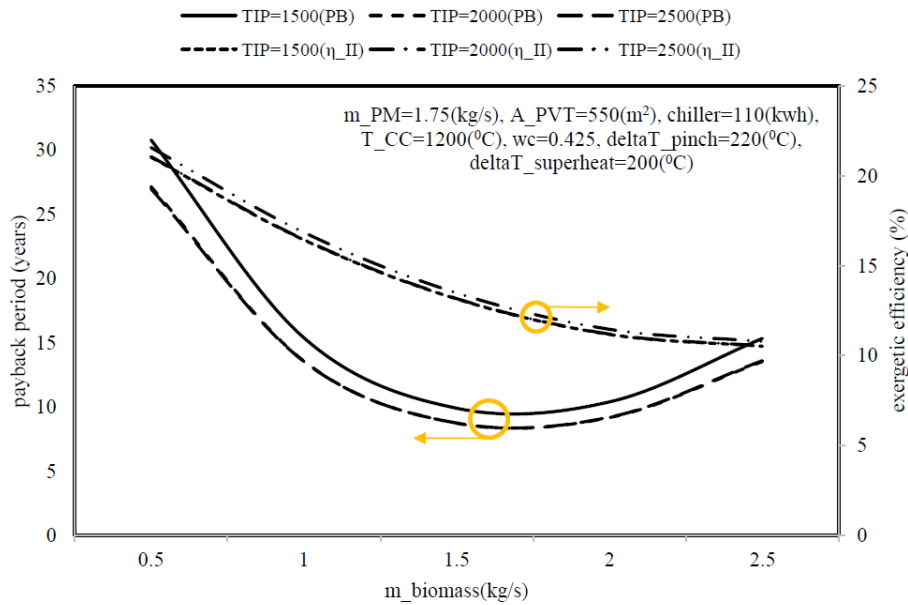


Fig. 15. Impact of biomass consumption and turbine inlet pressure on payback period and exergy efficiency.

4 Conclusions

In this study, the objective was to enhance the performance of the Combined cooling, heating, and power (CCHP) cycle by considering the payback period and exergy efficiency. Initially, each component of the cycle was verified by comparing it with relevant literature, and the outcomes of this validation process were

presented. The paper also presents the results of multi-objective optimization. When focusing solely on minimizing the payback period, the cycle can be configured to achieve a minimum payback period of 3.82 years. On the other hand, if the goal is to maximize system efficiency, the system can be adjusted to reach a maximum efficiency of 24.7. In cases where both efficiency and a short payback period are desired, the multi-objective optimization results indicate that a system with an optimized efficiency of 27 percent will have a

payback period of 4.8 years.

Also, the effect of several performance parameters of the cycle of exergy efficiency and payback period has been studied. Results indicates that the most impact is caused by the biomass consumption rate due to lower efficiency of this system compare to other components. Another parameter is turbine inlet pressure that has a massive impact on payback period and little impact on exergy efficiency. Also, as cooling capacity of the cycle increases the payback period due to the fact that cost of

cooling capacity produced by absorption cycle is high. In the present work biomass was utilized for powering the cycle. In future works the effect of utilizing other renewable energy sources such as wind or geothermal can be studied. As stated earlier the aim of the present work is to minimize the cost of the cooling cycle which can be achieved with optimizing the refrigeration cycle or utilizing more advanced refrigeration technologies. The current study shows that the cost of cooling cycle is relatively high which needs to be alleviated.

Table 4. Exergy destruction rate equation for each component.

Component	Exergy Destruction	Component	Exergy Destruction
Anaerobic Digester	$\dot{E}_{D,dig} = \dot{E}_5 + \dot{E}_6 - \dot{E}_7 - \dot{E}_{8a}$	Expansion Valve 2	$\dot{E}_{D,exv2} = \dot{E}_{24} - \dot{E}_{25}$
Combustion Chamber	$\dot{E}_{D,cc} = \dot{E}_8 + \dot{E}_9 - \dot{E}_{10a}$	Absorption Cycle Pump	$\dot{E}_{D,PRef} = \dot{W}_{rp} - (\dot{E}_{21} - \dot{E}_{20})$
Combustion Gases Exhaust Fan	$\dot{E}_{D,ExF} = \dot{W}_{ExF} - (\dot{E}_{11c} - \dot{E}_{11})$	PVT	$\dot{E}_{D,coll} = \dot{E}_{S,abs} - (\dot{E}_{31} + \dot{W}_{coll})$
Rankine Cycle Pump	$\dot{E}_{D,Pr} = \dot{W}_{Pr} - (\dot{E}_2 - \dot{E}_1)$	Pasteurizer	$\dot{E}_{D,pas} = (\dot{E}_{32} - \dot{E}_{33}) - (\dot{E}_{27} - \dot{E}_{26})$
Steam Turbine	$\dot{E}_{D,st} = \dot{E}_3 - \dot{E}_4 - \dot{W}_{st}$	Absorption Cycle Cooler	$\dot{E}_{D,coolRef} = (\dot{E}_{14} - \dot{E}_{15}) - (\dot{E}_{29} - \dot{E}_{28})$
Steam Generator	$\dot{E}_{D,sg} = \dot{E}_2 + \dot{E}_{10} - \dot{E}_3 - \dot{E}_{11a}$	Dryer Evaporator	$\dot{E}_{D,EvaPM} = (\dot{E}_{30a} - \dot{E}_{30b}) - (\dot{E}_{42} - \dot{E}_{27}) - \dot{E}_{30c}$
Rankine Condenser	$\dot{E}_{D,CondR} = \dot{E}_{12} + \dot{E}_4 - \dot{E}_1 - \dot{E}_{13}$	Dryer Pump	$\dot{E}_{D,PPM} = (\dot{E}_{43} - \dot{E}_{42}) - \dot{W}_{PPM}$
Absorption Cycle Generator	$\dot{E}_{D,GRef} = \dot{E}_{22} - \dot{E}_{16} - \dot{E}_{23} + \dot{E}_{34} - \dot{E}_{35}$	Dryer Cooler	$\dot{E}_{D,coolPM} = (\dot{E}_{45} - \dot{E}_{44}) - (\dot{E}_{47} - \dot{E}_{46})$
Absorption Cycle Condenser	$\dot{E}_{D,ConRef} = \dot{E}_{16} + \dot{E}_{38} - \dot{E}_{39} - \dot{E}_{17}$	Dryer Economizer	$\dot{E}_{D,eco} = (\dot{E}_{55} - \dot{E}_{54}) - (\dot{E}_{48} - \dot{E}_{47})$
Absorption Cycle Evaporator	$\dot{E}_{D,EvaRef} = \dot{E}_{18} + \dot{E}_{36} - \dot{E}_{19} - \dot{E}_{37}$	Dryer Fan	$\dot{E}_{D,fanPM} = \dot{W}_{fanPM} - (\dot{E}_{49} - \dot{E}_{48})$
Absorption Cycle Absorber	$\dot{E}_{D,absRef} = \dot{E}_{19} + \dot{E}_{40} + \dot{E}_{25} - \dot{E}_{20} - \dot{E}_{41}$	Dryer Heater	$\dot{E}_{D,heat} = \dot{E}_{50a} - \dot{E}_{50b} - (\dot{E}_{50} - \dot{E}_{49} + \dot{E}_{50c})$
Absorption Cycle heat Exchanger	$\dot{E}_{D,ExRef} = \dot{E}_{21} - \dot{E}_{22} + \dot{E}_{23} - \dot{E}_{24}$	Dryer Compressor	$\dot{E}_{D,comp} = \dot{W}_{comp} - (\dot{E}_{53} - \dot{E}_{52})$
Expansion Valve 1	$\dot{E}_{D,exv1} = \dot{E}_{18} - \dot{E}_{17}$	Dryer	$\dot{E}_{D,drier} = (\dot{E}_{53} + \dot{E}_{51} - \dot{E}_{54}) - (\dot{E}_{44} - \dot{E}_{43})$

Table 5. Exergy-economic equation for each component.

Component	Exergy-Economic Equation	Exergy-Economic Equation
Anaerobic Digester	$\dot{C}_7 + \dot{Z}_{dig} = \dot{C}_8$	$\dot{C}_{18} + \dot{C}_{15} + \dot{Z}_{EvaRef} = \dot{C}_{20} + \dot{C}_{41}, c_{25} = c_{20}, c_{40} = c_{41}$
Combustion Chamber	$\dot{C}_8 + \dot{C}_9 + \dot{Z}_{cc} = \dot{C}_{10}$	$\dot{C}_{14} + \dot{C}_{28} + \dot{Z}_{coolRef} = \dot{C}_{15} + \dot{C}_{29}, c_{14} = c_{15}, c_{28} = c_{29}$

Table 6. Exergy-economic equation for each component.

Component	Exergy-Economic Equation	Component	Exergy-Economic Equation
Anaerobic Digester	$\dot{C}_7 + \dot{Z}_{\text{dig}} = \dot{C}_8$	Absorption Cycle Absorber	$\dot{C}_{18} + \dot{C}_{15} + \dot{Z}_{\text{EvaRef}} = \dot{C}_{15} + \dot{C}_{41}$, $c_{25} = c_{20}, c_{40} = c_{41}$
Combustion Chamber	$\dot{C}_8 + \dot{C}_9 + \dot{Z}_{\text{cc}} = \dot{C}_{10}$	Absorption Cycle Evaporator	$\dot{C}_{14} + \dot{C}_{28} + \dot{Z}_{\text{coolRef}} = \dot{C}_{15} + \dot{C}_{29}$, $c_{14} = c_{15}, c_{28} = c_{29}$
Rankine Cycle Pump	$\dot{C}_1 + \dot{Z}_{\text{Pr}} + \dot{C}_{W,\text{Pr}} = \dot{C}_2$, $c_{W,\text{Pr}} = c_{W,\text{st}}, c_1 = c_2$	PVT	$\dot{Z}_{\text{Sol}} = \dot{C}_{31} + \dot{W}_{\text{Sol}}$, $c_{w,\text{Sol}} = c_{w,\text{Pr}}$
Steam Turbine	$\dot{C}_3 + \dot{Z}_{\text{st}} = \dot{W}_{\text{st}} + \dot{C}_4, c_4 = c_3$	Pasteurizer	$\dot{C}_{32} + \dot{C}_{26} + \dot{Z}_{\text{pas}} = \dot{C}_{33} + \dot{C}_{27}$, $c_{32} = c_{33}, c_{26} = c_{27}$
Steam Generator	$\dot{C}_2 + \dot{C}_{10} + \dot{Z}_{\text{sg}} = \dot{C}_{11} + \dot{C}_3$, $c_{11} = c_{10}$	Dryer Evaporator	$\dot{C}_{27} + \dot{C}_{30a} + \dot{Z}_{\text{EvaPM}} =$ $\dot{C}_{30c} + \dot{C}_{30b} + \dot{C}_{42}, c_{30a} = c_{30b}$, $c_{27} = c_{42}$
Rankine Condenser	$\dot{C}_4 + \dot{C}_{12} + \dot{Z}_{\text{CondR}} = \dot{C}_{13} + \dot{C}_1$, $c_4 = c_1$	Milk Powder Pump	$\dot{C}_{42} + \dot{Z}_{\text{PPM}} + \dot{C}_{w,\text{PPM}} = \dot{C}_{43}$, $c_{42} = c_{43}, c_{w,\text{PPM}} = c_{w,\text{Pr}}$
Exhaust Fan	$\dot{C}_{48} + \dot{Z}_{\text{ExF}} + \dot{C}_{W,\text{ExF}} = \dot{C}_{49}$, $c_{W,\text{ExF}} = c_{W,\text{Pr}}, c_{48} = c_{49}$	Dryer Economizer	$\dot{C}_{47} + \dot{C}_{54} + \dot{Z}_{\text{eco}} = \dot{C}_{48} + \dot{C}_{55}$, $c_{47} = c_{48}, c_{54} = c_{55}$
Absorption Cycle Generator	$\dot{C}_{22} + \dot{C}_{34} + \dot{Z}_{\text{GRef}} =$ $\dot{C}_{16} + \dot{C}_{23} + \dot{C}_{35}, c_{34} = c_{35}$	Dryer Fan	$\dot{C}_{48} + \dot{Z}_{\text{fanPM}} + \dot{C}_{w,\text{fanPM}} = \dot{C}_{49}$, $c_{48} = c_{49}, c_{w,\text{fanPM}} = c_{w,\text{Pr}}$
Absorption Cycle Condenser	$\dot{C}_{16} + \dot{C}_{38} + \dot{Z}_{\text{ConRef}} = \dot{C}_{17} + \dot{C}_{39}$, $c_{16} = c_{17}, c_{38} = c_{39}$	Dryer Compressor	$\dot{C}_{52} + \dot{Z}_{\text{comp}} + \dot{C}_{w,\text{comp}} = \dot{C}_{53}$, $c_{52} = c_{53}, c_{w,\text{comp}} = c_{w,\text{Pr}}$
Absorption Cycle Heat Exchanger	$\dot{C}_{21} + \dot{C}_{23} + \dot{Z}_{\text{ExRef}} = \dot{C}_{22} + \dot{C}_{24}$, $c_{21} = c_{22}, c_{23} = c_{24}$	Dryer Heater	$\dot{C}_{49} + \dot{C}_{50a} + \dot{Z}_{\text{heat}} =$ $\dot{C}_{50} + \dot{C}_{50b} + \dot{C}_{50c}, c_{50a} = c_{50b}$
Absorption Cycle Pump	$\dot{C}_{21} + \dot{Z}_{\text{pRef}} + \dot{C}_{w,\text{pRef}} = \dot{C}_{22}$, $c_{21} = c_{22}, c_{w,\text{pRef}} = c_{w,\text{Pr}}$	Dryer Fan	$\dot{C}_{53} + \dot{C}_{43} + \dot{C}_{51} + \dot{Z}_{\text{drier}} =$ $\dot{C}_{44} + \dot{C}_{54}$
Absorption Cycle Absorber	$\dot{C}_{19} + \dot{C}_{25} + \dot{C}_{40} + \dot{Z}_{\text{absRef}} =$ $\dot{C}_{20} + \dot{C}_{41}, c_{25} = c_{20}, c_{40} = c_{41}$	Dryer Cooler	$\dot{C}_{46} + \dot{C}_{44} + \dot{Z}_{\text{coolPM}} = \dot{C}_{47} + \dot{C}_{45}$, $c_{44} = c_{45}, c_{46} = c_{47}$

Table 7. Capital cost Equation for each component of the cycle [11, 12].

Component	Capital Cost Estimation	Remarks
Anaerobic Digester	$Z_{\text{dig}} = 35000 \left(\frac{VT}{21000} \right)^{0.75}$	V : Volumetric Flow Rate T : Working Temperature
Combustion Chamber	$Z_{\text{cc}} = c_1 \dot{m}_{\text{air}} [1 + \exp(c_2 T_{\text{out}} - c_3)]$ $\times \frac{1}{0.995 - \frac{P_{\text{out}}}{P_{\text{in}}}}$, $c_1 = 48.64 \text{ \$/ (kg/s)}, c_2 = 0.18 \text{ K}^{-1}, c_3 = 26.4$	T_{out} : Outlet temperature of combustion chamber $\frac{P_{\text{out}}}{P_{\text{in}}}$: pressure ratio of combustion chamber
Rankine Cycle Pump	$Z_{\text{Pr}} = c_4 (\dot{W}_{\text{Pr}})^{0.71}, c_4 = 3540 \text{ \$/kw}^{0.71}$	\dot{W}_{Pr} : Pump Brake Horse Power
Steam Turbine	$Z_{\text{st}} = c_5 (\dot{W}_{\text{st}})^{0.7}, c_5 = 6000 \text{ \$/kw}^{0.7}$	\dot{W}_{st} : Turbine Output Power
Rankine Condenser	$Z_{\text{CondR}} = c_9 \dot{m}_{\text{water}}, c_9 = 1773 \text{ \$/ (kg/s)}$	\dot{m}_{water} : Water mass Flow rate
Exhaust Fan	$Z_{\text{ExF}} = 2833 (\dot{m}_{\text{exG}})^{0.7053}$	\dot{m}_{exG} : Exhaust Gas Mass Flow rate
Absorption Cycle Generator	$Z_{\text{GRef}} = 17500 \left(\frac{A_{\text{gen}}}{100} \right)^{0.06}$	A_{gen} : Surface Area of Generator

Table 7. Capital cost Equation for each component of the cycle [11, 12] (Continued).

Component	Capital Cost Estimation	Remarks
Steam Generator	$Z_{sg} = 6570 \left[\left(\frac{\dot{Q}_{ec}}{\Delta T_{lm,ec}} \right)^{0.8} + \left(\frac{\dot{Q}_{ev}}{\Delta T_{lm,ev}} \right)^{0.8} \right] + 21276\dot{m}_s + 1184.4\dot{m}_g^{1.2}$	$\Delta T_{lm,ec}$: Temperature Difference of inlet and outlet Gas $\Delta T_{lm,ev}$: Temperature Difference of water inlet and steam outlet Q_{ec} : Gas heat transfer Q_{ev} : Steam heat transfer \dot{m}_s : Steam mas flow rate \dot{m}_g : Gas mass flow rate
Absorption Cycle Condenser	$Z_{ConRef} = c_9\dot{m}_{water}$, $c_9 = 1773\$/kg/s$	\dot{m}_{water} : Water mass Flow Rate
Absorption Cycle Heat Exchanger	$Z_{ExRef} = 4760A_{ex}^{0.68}$	A_{ex} : Surface Area of Heat Exchanger
Absorption Cycle Pump	$Z_{PRef} = c_4(\dot{W}_{PRef})^{0.71}$, $c_4 = 3540\$(kw)^{0.71}$	\dot{W}_{PRef} : Pump Brake Horse Power
Absorption Cycle Absorber	$Z_{AbsRef} = 16000 \left(\frac{A_{abs}}{100} \right)^{0.06}$	A_{abs} : Surface Area of Absorber
Absorption Cycle Evaporator	$Z_{EvaRef} = 16000 \left(\frac{A_{eva}}{100} \right)^{0.06}$	A_{eva} : Surface Area of Evaporator
Absorption Cycle Cooler	$Z_{coolRef} = 4760A_{cool}^{0.68}$	A_{cool} : Surface Area of Cooler
PVT	$Z_{PVT} = 310A_{PVT}$	A_{PVT} : Surface Area of PVT Exposed to Sun
Pasteurizer	$Z_{Pas} = 4680(A_{Pas})^{0.742}$	A_{Pas} : Surface Area of Pasturized
Milk Powder Cycle Evaporator	$Z_{EvaPM} = 51733 \ln(A_{evaPM}) - 74437$	A_{evaPM} : Surface Area of Evapoprator
Milk Powder Cycle Pump	$Z_{PPM} = 5870(\dot{W}_{PPP})^{0.85}$	\dot{W}_{PPP} : Pump Brake Horse Power
Milk Powder Cycle Economizer	$Z_{eco} = 1644A_{eco}^{0.81} + 18900$	A_{eco} : Surface Area of Economizer
Milk Powder Cycle Blower	$Z_{fanPM} = 2833(\dot{m}_{airPM})^{0.7053}$	\dot{m}_{airPM} : Mass Flow Rate of Air
Compressor	$Z_{AC} = \left(\frac{c_{10}\dot{m}_{air}}{c_{11} - \eta_{is,AC}} \right) \left(\frac{P_{out}}{P_{in}} \right) \ln \frac{P_{out}}{P_{in}}$ $c_{10} = 75 s/kg$, $c_{11} = 0.9$	\dot{m}_{air} : Mass flow rate of air $\frac{P_{out}}{P_{in}}$: Compressor Pressure Ratio
Milk Powder Cycle Heater	$Z_{heat} = 1644A_{heat}^{0.81} + 18900$	A_{heat} : Surface Area of Heater
Milk Powder Cycle Dryer	$Z_{drier} = 35800(\dot{m}_{\pm})^{0.3048}$	\dot{m}_{\pm} : Mass Flow Rate of Milk Powder
Milk Powder Cycle Cooler	$Z_{coolPM} = 5430A_{coolPM}^{0.7}$	A_{coolPM} : Surface Area of Cooler

Acknowledgements

This research was supported by Iranian Fuel Conservation Company (IFCO). Authors appreciate colleagues

of research and development as well as energy optimization in building departments who provided insight and expertise that assisted the research.

Nomenclature

\dot{m}	Mass flow rate (kg/s)
Q	Heat transfer (kW)
Z	Exergy-Economic Factor
T_{amb}	Ambient temperature (°C or K)
P	Pressure (bar)
\dot{W}	Work (kW)
T	Temperature of component (°C or K)
η	Exergy efficiency (%)
Ψ	Exergy efficiency (%)

References

- [1] Musharavati F, Khoshnevisan A, Alirahmi SM, Ahmadi P, Khanmohammadi S. Multi-objective optimization of a biomass gasification to generate electricity and desalinated water using Grey Wolf Optimizer and artificial neural network. *Chemosphere*. 2022;287:131980. [272](#)
- [2] Rezvan AT, Gharneh NS, Gharehpetian G. Robust optimization of distributed generation investment in buildings. *Energy*. 2012;48(1):455–463. [272](#)
- [3] Chlipała M, Błaszczak P, Wang SF, Jasiński P, Bochentyn B. In situ study of a composition of outlet gases from biogas fuelled Solid Oxide Fuel Cell performed by the Fourier Transform Infrared Spectroscopy. *International Journal of Hydrogen Energy*. 2019;44(26):13864–13874. [272](#)
- [4] Pantaleo AM, Camporeale SM, Miliozzi A, Russo V, Shah N, Markides CN. Novel hybrid CSP-biomass CHP for flexible generation: Thermo-economic analysis and profitability assessment. *Applied energy*. 2017;204:994–1006. [272](#), [274](#)
- [5] Nazari N, Mousavi S, Mirjalili S. Exergo-economic analysis and multi-objective multi-verse optimization of a solar/biomass-based trigeneration system using externally-fired gas turbine, organic Rankine cycle and absorption refrigeration cycle. *Applied Thermal Engineering*. 2021;191:116889. [273](#)
- [6] Saini P, Singh J, Sarkar J. Thermodynamic, economic and environmental analyses of a novel solar energy driven small-scale combined cooling, heating and power system. *Energy Conversion and Management*. 2020;226:113542. [274](#)
- [7] Worawimut C, Vivanpatarakij S, Watanapa A, Wiyaratn W, Assabumrungrat S. Performance evaluation of biogas upgrading systems from swine farm to biomethane production for renewable hydrogen source. *International Journal of Hydrogen Energy*. 2019;44(41):23135–23148. [274](#)
- [8] Abdeshahian P, Lim JS, Ho WS, Hashim H, Lee CT. Potential of biogas production from farm animal waste in Malaysia. *Renewable and Sustainable Energy Reviews*. 2016;60:714–723. [274](#)
- [9] Gürlich D, Dalibard A, Eicker U. Photovoltaic-thermal hybrid collector performance for direct trigeneration in a European building retrofit case study. *Energy and Buildings*. 2017;152:701–717. [275](#)
- [10] Joshi A, Tiwari A, Tiwari G, Dincer I, Reddy B. Performance evaluation of a hybrid photovoltaic thermal (PV/T)(glass-to-glass) system. *International Journal of Thermal Sciences*. 2009;48(1):154–164. [275](#), [276](#)
- [11] Buswell AM. Anaerobic fermentations. *Bulletin (Illinois State Water Survey) no 32*. 1939;. [276](#), [282](#), [283](#)
- [12] Wellinger A, Murphy JD, Baxter D. *The biogas handbook: science, production and applications*. Elsevier; 2013. [276](#), [277](#), [282](#), [283](#)
- [13] Din I, Rosen MA, Ahmadi P, et al. *Optimization of energy systems*. John Wiley & Sons; 2017. [276](#)
- [14] Bejan A, Tsatsaronis G, Moran MJ. *Thermal design and optimization*. John Wiley & Sons; 1995. [276](#)
- [15] Behzadi A, Houshfar E, Gholamian E, Ashjaee M, Habibollahzade A. Multi-criteria optimization and comparative performance analysis of a power plant fed by municipal solid waste using a gasifier or digester. *Energy Conversion and Management*. 2018;171:863–878. [276](#), [277](#)
- [16] Soltani S, Mahmoudi S, Yari M, Morosuk T, Rosen M, Zare V. A comparative exergoeconomic analysis of two biomass and co-firing combined power plants. *Energy Conversion and Management*. 2013;76:83–91. [276](#)
- [17] Aman J, Ting DK, Henshaw P. Residential solar air conditioning: Energy and exergy analyses of an ammonia–water absorption cooling system. *Applied Thermal Engineering*. 2014;62(2):424–432. [277](#)